A Market-Based Resilient Power Management Technique for Distribution Systems with Multiple Microgrids Using a Multi-Agent System Approach

Authors: Kaveh Dehghanpour and Hashem Nehrir

This is an Accepted Manuscript of an article published in Electric Power Components and Systems on January 24, 2019, available online: http://www.tandfonline.com/doi/full/10.1080/15325008.2018.1527869.

Dehghanpour, Kaveh, and Hashem Nehrir. “A Market-Based Resilient Power Management Technique for Distribution Systems with Multiple Microgrids Using a Multi-Agent System Approach.” Electric Power Components and Systems (January 24, 2019): 1–12. doi:10.1080/15325008.2018.1527869.

A Market-Based Resilient Power Management Technique for Distribution Systems with Multiple Microgrids Using a Multi-Agent System Approach

Kaveh Dehghanpour and Hashem Nehrir
ECE Department, Montana State University, Bozeman, Montana, USA

CONTENTS

Abstract—In this paper, we present a market-based resilient power management procedure for electrical distribution systems consisting of multiple cooperative MiroGrids (MGs). Distributed optimization is used to find the optimal resource allocation for the multiple MG system, while maintaining the local and global constraints, including keeping the voltage levels of the micro-sources within bounds. The proposed method is based on probabilistic reasoning in order to consider the uncertainty of the decision model in preparation for expected extreme events and in case of unit failure, to improve the resiliency of the system. Basically, the power management problem formulation is a multiobjective optimization problem, which is solved using the concept of Nash Bargaining Solution (NBS). The simulation results show that the proposed method is able to improve the resiliency of the system and prepare it for extreme events and unit failure, by increasing power reserve and modifying the operating point of the system to maintain voltage and power constraints across the MGs.

1. INTRODUCTION

Power system resiliency is defined as the grid's ability to withstand high impact disruptive events (*e.g.*, storms, hurricanes, etc.), while continuing to provide energy to critical loads, and restoring services to all consumers after the events, as fast as possible [1]. Hence, as discussed in [2], a crucial aspect of resilient power systems depends on how the designed control and power management systems within the grid respond to these extreme events. Also, as shown in [3], a systemic long-term approach, spanning various agencies and departments, is required to ensure the resiliency of a complex and critical infrastructure, such as the US national grid.

To improve the resiliency of the power systems some levels of micro-generation and distributed/local decision-making capabilities should be integrated into power systems. In this respect, the concept of self-sufficient MicroGrids (MGs) becomes highly relevant, given the

ability of MGs to continue providing service to the consumers in islanded mode. Also, MGs provide an efficient framework for introducing distributed and local control and power management capabilities in distribution systems, which can be exploited to decentralize the decision-making procedures in power systems and avoid single-point-of-failure.

The connection between MG operation and resiliency enhancement has been studied in several papers. A non-cooperative game theoretic model is proposed in [4] to address the strategic behavior of MGs, using the concept of Nash equilibrium. Different failure modes are considered in the paper to improve the resiliency of the system. A two-stage resiliency-oriented decision model is presented in [5] for a single MG to mitigate the effect of service interruption, using a stochastic programing technique. Also, in [6] different indexes are introduced to assess the resiliency of power systems consisting of MGs, employing Markov model and Monte Carlo simulation. In [7], MGs are used as resiliency resource (both at local and community levels). A self-healing strategy is proposed in [8] for two neighboring MGs to support each other in times of load deficiency. A self-healing agent is considered that is able to operate in both centralized and decentralized modes. A centralized resiliency-oriented MG scheduling is proposed in [9] for a single MG, which enables it to operate in grid-connected and islanded modes. Another resiliency-based power control scheme for multi-MG systems is proposed in [10], where at the global level a distributed resource allocation problem is solved, whereas at local levels, the scheduling problems are solved centrally within each MG.

In [11], we employed the concept of Nash Bargaining Solution (NBS) to develop a distributed agent-based Multi-Objective (MO) power management framework for a single MG. Within this framework, the control agents of the different micro-sources of the MG interact with each other to solve a resource allocation problem and reach a unique, Pareto-optimal, and fair solution, employing the Distributed Sub-Gradient Algorithm (DSGA) [12, 13]. The DSGA is a distributed optimization technique, through which a number of agents are able to collectively solve a global optimization problem, only with access to local and private data. In [14], this decision model was extended to multi-MG power distribution systems, by introducing additional layers to the bargaining hierarchy. Also, the impact of interaction of the multi-MG network with a retail market agent on system operation and energy pricing were studied.

This paper presents a multi-MG power management scheme and evaluates the resiliency of the system by "preparing" it for extreme events and unit failure, well ahead of time, for look-ahead decision horizons, based on forecasted probability of event occurrence. To obtain a pre-event preparedness, a new objective function is introduced to the decision problem of each MG. The purpose of this objective function is to minimize the expected loss of load for certain look-ahead times during system operation, based on the predicted chances of unit failure and blackout in the main grid. Thus, we assume that each MG has access to a probabilistic overview of the structure of the system and the environmental conditions around the location of the MG for different look-ahead times (*e.g.*, probability of islanding and unit failure due to extreme events). This probability gets updated as the decision window rolls along with time. This probabilistic overview basically represents the agents' "belief" on the future state of the system. Employing this probabilistic model, the agents perform reserve allocation to minimize the chance of service disruption to consumers. This probabilistic objective function is integrated within the distributed decision model. Simulations have been performed with and without the proposed objective function to compare the outcomes of our proposed resiliency-aware power management with the original power management scheme. Also, the model is extended to include the constraints on the voltage magnitude of each micro-source, including the controllable load bus, to maintain them within permissible bounds. Voltage constraints and reactive power allocation are considered in the distributed optimization model, using a convex relaxation of AC power flow [15]. This is achieved by adding reactive power to the decision vector of the micro-sources of the MGs. Different components of the system can be affected during an extreme event (*e.g.*, cables, conductor lines, micro-sources, control system, and communication links). However, the focus of this paper is to evaluate the behavior of the system under islanding and micro-source failure scenarios. An advantage of using the DSGA is that the algorithm is able to converge even for time-varying interaction networks. Hence, even if certain controllers or communication links fail after an event, the rest of the agents that are connected to each other can still find a near-optimal point of operation for their respective micro-sources. To summarize, the contributions of the paper are as follows:

- A game-theoretic agent-based power management system is designed to coordinate active/reactive power of different resources for multiple MGs in a regional distribution systems to achieve local objectives and enforce constraints.

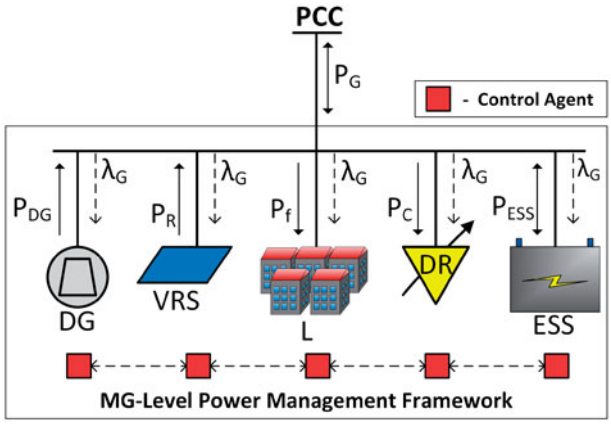

FIGURE 1. Structure of an MG used in the paper.

- The proposed decision model has been modified to include probabilistic objective functions for incorporating resiliency enhancement. A probabilistic framework has been designed to model reserve allocation in "preparation" for extreme events and unit failure to enhance the resiliency of the network against these events.

2. DISTRIBUTED BARGAINING FRAMEWORK FOR MULTIPLE MGS

In this section, we give a brief review of the distributed bargaining procedure, which takes advantage of the concept of NBS. The basic idea of this method is that a community of cooperative agents within multiple MGs, with different sets of objective functions and constraints, negotiate with each other to reach a unique, fair, and Pareto-optimal solution. As shown in [16], NBS satisfies these desirable properties. Moreover, NBS can be found through a distributed optimization mechanism, due to its distributed-sum structure [11, 12]. In this paper, we assign a Photo-Voltaic (PV) unit, a Dispatchable Generator (DG) unit, an Energy Storage System (ESS), uncontrollable and curtailable Demand Response (DR) resources to each MG, as shown in Figure 1 [11]. A separate control agent is considered for each micro-source (*i.e.*, the DG, ESS, and DR resources of each MG). Also, a main control agent is in charge of controlling each MG's net power exchange with the main grid, at the Point of Common Coupling (PCC). The PV unit is operated based on the concept of maximum power point tracking; the unit's output power is simply predicted and used as input to the decision problem, based on calculated prediction error distribution discussed in [17]. However, we assume that the PV systems have limited amount of controllable reactive power (due to storage elements at their DC buses), which is controlled by a local agent for voltage regulation at the PV buses. The following objective functions and constraints are considered for the control agents of the micro-sources and main control agent (at the PCC) of each MG, where, $U_{j,i}^m$ indicates the j^{th} objective function of the i^{th} micro-source of the m^{th} MG:

- DG control agent:

$$U_{1,1}^m = \sum_{t=1}^{H} \Big\{ -P_G^m(t)\lambda_R(t) - \Big(a^m P_{DG}^m(t)^2 + b^m P_{DG}^m(t) + c^m\Big) \Big\} \tag{1}$$

$$U_{2,1}^m = \frac{1}{H}\sum_{t=1}^{H} \frac{k \cdot P_{DG}^m(t)}{a^m P_{DG}^m(t)^2 + b^m P_{DG}^m(t) + c^m} \tag{2}$$

$$P_{DG}^{\min,m} \le P_{DG}^m(t) \le P_{DG}^{\max,m} \tag{3}$$

$$|P_{DG}^m(t) - P_{DG}^m(t-1)| \le GRC^m \cdot \Delta t \tag{4}$$

$$S_{DG}^m(t) = \sqrt{\big(P_{DG}^m(t)\big)^2 + \big(Q_{DG}^m(t)\big)^2} \tag{5}$$

$$0 \le S_{DG}^m(t) \le S_{DG}^{\max,m} \tag{6}$$

$$V_{DG}^{\min,m} \le |V_{DG}^m(t)| \le V_{DG}^{\max,m} \tag{7}$$

$$|V_{DG}^m(t)| \approx 1 + \sum\nolimits_{j\in\aleph_{DG}} \{R_{DG,j}P_{DG,j} + X_{DG,j}Q_{DG,j}\} \tag{8}$$

where, $U_{1,1}^m$ and $U_{2,1}^m$ represent the profitability of local power generation and average efficiency of operation, respectively. Also, $P_G^m(t)$ denotes the m^{th} MG's power import from the grid (at the retail price $\lambda_R(t)$). Note that $P_G^m \le 0$ represents power export to the grid. Coefficients a^m, b^m, and c^m define the quadratic cost function of the DG [18], and $P_{DG}^m(t)$ denotes the output power of the DG unit of the m^{th} MG. Constraint (3) maintains the acceptable minimum and maximum power output levels of the DG unit ($[P_{DG}^{\min,m}, P_{DG}^{\max,m}]$). Also, (4) enforces the Generation Rate Constraint (GRC) of the DG unit. In this paper, H, t, and Δt denote the length of the decision window, time instant, and decision time step value, respectively. The apparent power of the DG, S_{DG}^m, is defined in (5) as a function of the DG's active and reactive power ($Q_{DG}^m(t)$) and is maintained within its boundaries ($[0, S_{DG}^{\max,m}]$) through (6). To enforce the local voltage constraint (7) on the DG's bus voltage magnitude ($V_{DG}^m(t)$), a convex relaxation of AC power flow is adopted from [15] and shown in (8). This procedure is used for other micro-sources as well. Equation (8) is based on the simplifying assumption that the phase angle difference between the node voltages in distribution systems is small. The convexity of

the constraints is crucial to ensure that the NBS is well-defined [16]. Here, $\aleph_{DG}$ denotes the set of neighboring buses to the DG bus. $R_{DG,j}$ and $X_{DG,j}$ are the resistance and reactance values of the line connecting the DG bus to its j^{th} neighboring bus, respectively. Also, $P_{DG,j}$ and $Q_{DG,j}$ define the active and reactive power sent from the DG to its j^{th} neighboring bus. Other convex relaxations of the AC power flow found in the literature (*e.g.*, [19, 20]) can also be used in the decision problem.

- DR provider agent:

$$U_{1,2}^{m} = \frac{1}{H}\sum_{t=1}^{H} \lambda_R(t) \cdot P_f^m(t) \cdot \left(1 - \exp\left\{-\omega^m\left(P_f^m(t) - P_C^m(t)\right)\right\}\right) \tag{9}$$

$$U_{2,2}^{m} = \sum_{t=1}^{H} -P_C^m(t)\lambda_R(t) \tag{10}$$

$$P_C^{\min,m} \le P_C^m(t) \le P_C^{\max,m} \tag{11}$$

$U_{1,2}^m$ and $U_{2,2}^m$ represent penalty for load reduction [21], and cost-savings, respectively, as two competing objective functions for DR management. Thus, deviations from the target (forecasted) fixed load value $P_f^m(t)$) are penalized through $U_{1,2}^m$, depending on the aggregate participation factor, ω^m. $P_C^m(t)$ defines the aggregate power of the curtailed load, and $[P_C^{\min,m}, P_C^{\max,m}]$ are the acceptable curtailment boundaries of the DR resources.

- ESS control agent:

$$P_{ESS}^{\min,m} \le P_{ESS}^m(t) \le P_{ESS}^{\max,m} \tag{12}$$

$$SOC^m(t) = SOC^m(t-1) - \frac{\Delta t}{E_{\max}} P_{ESS}^m(t) \tag{13}$$

$$SOC^{\min,m} \le SOC^m(t) \le SOC^{\max,m} \tag{14}$$

$$S_{ESS}^m(t) = \sqrt{\left(P_{ESS}^m(t)\right)^2 + \left(Q_{ESS}^m(t)\right)^2} \tag{15}$$

$$0 \le S_{ESS}^m(t) \le S_{ESS}^{\max,m} \tag{16}$$

$$V_{ESS}^{\min,m} \le |V_{ESS}^m(t)| \le V_{ESS}^{\max,m} \tag{17}$$

$$|V_{ESS}^m(t)| \approx 1 + \sum_{j\in\aleph_{ESS}} \{R_{ESS,j}P_{ESS,j} + X_{ESS,j}Q_{ESS,j}\} \tag{18}$$

the ESS control agents need to enforce constraints (12)-(18), where, (12) defines the minimum/maximum limits $[P_{ESS}^{\min,m}, P_{ESS}^{\max,m}]$) on the output power of the ESS unit ($P_{ESS}^m(t)$). Also, (13) and (14) describe the State Of Charge (SOC) computation and limitations ($[SOC^{\min,m}, SOC^{\max,m}]$) of the ESS, with $E_{\max,m}$ denoting the nominal energy capacity of the battery system in the m^{th} MG. Equations (15)–(18) enforce the local apparent power (S_{ESS}^m) and voltage magnitude ($|V_{ESS}^m(t)|$) constraints of the ESS, similar to the DG unit (with Q_{ESS}^m denoting the output reactive power of the ESS). Note that (18) is based on a "small voltage phase angle difference" assumption, similar to (8).

- PV control agent:

As discussed previously, the goal of the PV control agent is to maintain the local voltage and apparent power constraints of the PV bus, as follows:

$$S_{PV}^m(t) = \sqrt{\left(P_{PV}^m(t)\right)^2 + \left(Q_{PV}^m(t)\right)^2} \tag{19}$$

$$0 \le S_{PV}^m(t) \le S_{PV}^{\max,m} \tag{20}$$

$$V_{PV}^{\min,m} \le |V_{PV}^m(t)| \le V_{PV}^{\max,m} \tag{21}$$

$$V_{PV}^m(t) \approx 1 + \sum_{j\in\aleph_{PV}} \{R_{PV,j}P_{PV,j} + X_{PV,j}Q_{PV,j}\} \tag{22}$$

where, P_{PV}^m, Q_{PV}^m, and S_{PV}^m denote the active, reactive, and apparent output power of the PV system. Note that based on our assumption of maximum power point tracking for the PV system, P_{PV}^m is an input to the decision problem at different time steps. The constraints on the voltage of the PV bus V_{PV}^m) are shown in (21) and (22), using the small phase angle difference assumption, similar to the DG unit.

- Main MG control agent at the PCC:

$$U_{1,3}^{m} = \sum_{t=1}^{H} -\left(P_G^m(t)\right)^2 \tag{23}$$

$$P_G^{\min,m} \le P_G^m(t) \le P_G^{\max,m} \tag{24}$$

$$P_{Ex}^{max} \le \sum_{m=1}^{M} P_G^m(t) \le P_{Im}^{max,m} \tag{25}$$

$U_{1,3}^m$ is the objective function for the main MG agent (of the m^{th} MG). Its function is to promote self-sufficiency and avoid over-loading and congestion at the MG's PCC [22]. Constraint (24) defines the physical congestion limits of the m^{th} MG at the PCC ($[P_G^{\min,m}, P_G^{\max,m}]$). The system-wide power balance constraint is considered through (25), where $P_{Ex}^{\max}$ and $P_{Im}^{\max}$ define the maximum power export and import limits to the utility company, and M denotes the number of MGs in the Regional Energy Network (REN). Note that (25) only appears in the decision problem of the main MG agents at the PCC. This implies that the control agents of the micro-sources of the different MGs do not need to be connected together through communication links. Hence, only the control agents of the micro-sources within each MG are connected locally to their peers.

Apart from the introduced constraints, all the control agents of each MG need to enforce the local MG-wide power balance constraint in their decision model:

$$P_{DG}^m(t) + P_{PV}^m(t) + P_G^m(t) + P_{ESS}^m(t) + P_C^m(t) = P_f^m(t) \tag{26}$$

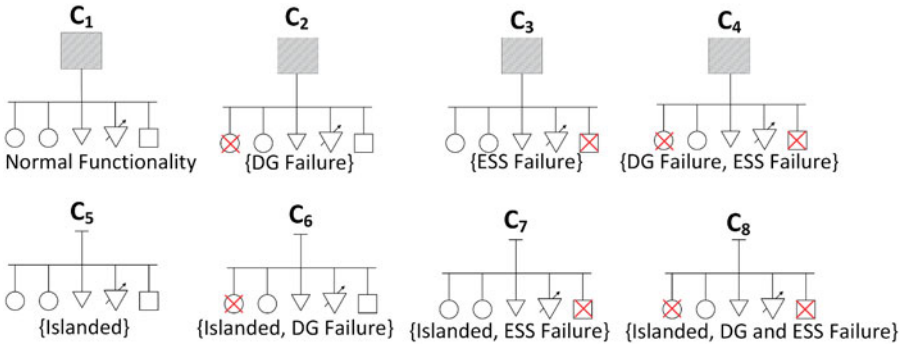

FIGURE 2. Different probable configurations for each MG, due to islanding and unit failure.

where, $P_f^m(t)$ is uncontrollable load level for the m^{th} MG. The overall cooperative resource allocation problem can be cast as NBS, as shown in our previous work [14]:

$$\max_{\boldsymbol{P},\boldsymbol{Q}} \sum_{m=1}^{M} \sum_{i=1}^{N_m} \log \prod_{j=1}^{O_i^m} \left(U_{j,i}^m - d_{j,i}^m\right) \quad (27)$$
$$s.t.\ (3)-(8),\ (11)-(22),\ (24)-(26) \forall m$$

where, $\boldsymbol{P}$ and $\boldsymbol{Q}$ are the decision vectors, containing the active and reactive power outputs of all controllable resources. N_m denotes the number of control agents of the m^{th} MG and O_i^m defines the number of objective functions of the i^{th} control agent in the m^{th} MG. Also, $d_{j,i}^m$'s represent the disagreement points of the bargaining process (i.e., worst case scenarios).

3. MAKING THE DISTRIBUTED BARGAINING FRAMEWORK RESILIENCY-AWARE

To introduce resiliency-awareness into the distributed optimization framework, we introduce a new objective function into the optimization problem (27). This objective function can be handled by a separate agent in each MG or the main control agent of every MG. The basic premise of this objective function is to minimize the expected power deficiency in case the MGs become islanded due to an extreme event, or if there is a unit failure in the system. Hence, we assume that an expert system or a forecasting unit is present at each MG to estimate the probability of MG islanding during extreme weather events. This probability value can also be given as an empirically evaluated input by the MG owners/operators. For instance, if there is an upcoming extreme event such as a hurricane or a storm in the area, the forecasting unit will assign a higher probability to the islanding scenario of the MGs since there is higher chance that a blackout will occur in the main grid. These probabilities can be estimated using statistical history of the system [23] and environmental parameters. Also, note that these probability values are time-varying, and change based on the state of the environment and weather. The time-variability of the probability value enables the operator to "prepare" the system against non-stationary extreme weather event.

The probabilities of different system configurations, consisting of component failure scenarios, shown in Figure 2, can be defined for each MG, as follows:

$$P\{C_i\} = \prod_{j=1}^{e_{C_i}} P\{E_j\} \quad (28)$$

where, C_i denotes the ith configuration, and E_i is an event belonging to the configuration's event set (consisting of e_{C_i} events). Also, $P\{\cdot\}$ defines the probability values of events/configurations. Note that the focus of this paper is not exactly scenario generation and reduction. We have assumed that another source (potentially a utility company) is providing the agents with probable practical scenarios. Since, each MG is a small-scale power system enumerating all the configurations is not numerically expensive. However, if the number of resources in the MG increases, we will be facing an exponential growth in the number of configurations, which can make enumeration impractical. In this case, scenario reduction can be performed to decrease the number of configurations. Different scenario reduction techniques have been proposed in the literature [24]. In this paper, we consider the following event set for each MG: {MG islanding, DG failure, ESS failure} to define operation scenarios. The probability set corresponding to this event set is defined (for the m^{th} MG) as: $\{p_{is}^m(t), p_{dg}^m(\mathrm{t}), p_{ess}^m(t)\}$. Hence, there are eight possible system configurations for each MG (Figure 2), with probability values defined as: $\{p_{C_1}^m(t), \ldots, p_{C_{c_{\max}}}^m(t)\}$, where $c_{\max}$ denotes the maximum number of configurations. Note that we have assumed that these events are statistically independent from each other. Thus, the objective function for improving system resiliency is defined as follows:

$$U_{2,3}^m = -\sum_{t=1}^{H} \sum_{i=1}^{C_{\max}} \left\{P_{Def}^m(t, C_i) - P_{Res}^m(\mathrm{t}, C_i)\right\} \cdot p_{C_i}^m(t) \quad (29)$$

This objective function represents the expected post-event power imbalance in each MG. Here, $P_{Def}^m(t, C_i)$ and

$P^m_{Res}(t, C_i)$ are the immediate power deficit level and total available power reserve at time t under system configuration C_i, for the m^{th} MG, respectively. Hence, through (29) the expected value of net power deficit is minimized. The main elements of this objective function are defined as follows:

$$P^m_{Def}(t, C_i) = r\Big\{P^m_f(t) - P^m_{DG}(t, C_i) - \mathrm{P}^m_{PV}(t) - P^m_{ESS}(t, C_i) - P^m_G(t, C_i) - P^m_C(t)\Big\} \tag{30}$$

$$P^m_{Res}(t, C_i) = P^m_{DG,Res}(t, C_i) + P^m_{ESS,Res}(t, C_i) + P^m_{G,Res}(t, C_i) + P^m_{C,Res}(t) \tag{31}$$

where, $r\{\cdot\}$ is the ramp function (*i.e.*, $r(x) = x$ for $x \geq 0$ and $r(x) = 0$ otherwise). The ramp function determines the immediate consumption deficit in the system. Also, $P^m_{DG,Res}(t, C_i)$, $P^m_{G,Res}(t, C_i)$, $P^m_{ESS,Res}(t, C_i)$, and $P^m_{C,Res}(t, C_i)$ define the available power reserve from the different micro-sources of each MG at different times and for different configurations. For each micro-source, the reserve level is a function of the operating point, and power and energy capacity of the source:

$$P^m_{DG,Res}(t, C_i) = \min\left(P^{\max,m}_{DG} - P^m_{DG}(t, C_i), GRC^m \cdot \Delta t\right) \tag{32}$$

$$P^m_{G,Res}(t, C_i) = P^{\max,m}_G - P^m_G(t, C_i) \tag{33}$$

$$P^m_{ESS,Res}(t, C_i) = \min\left(P^{\max,m}_{ESS} - P^m_{ESS}(t, C_i), \frac{E(t, C_i) - E^{\min,m}}{\Delta t}\right) \tag{34}$$

$$P^m_{C,Res}(t, C_i) = P^{\max,m}_C - P^m_C(t) \tag{35}$$

where, the $\min(a, b)$ operator selects the smaller number among its operands. $E(t, C_i)$ and $E^{\min,m}$ denote the available and minimum allowable energy levels of the ESS unit (*i.e.*, SOC), respectively. Note that based on (32) the available reserve from the DG is limited by its ramp rate constraint and maximum power capacity. Also, the reserve from the ESS unit is constrained by its maximum power capacity and minimum SOC limit, as can be seen in (34).

Considering (30)–(35), we observe that the objective function (29) is not differentiable at all points in the decision space. Hence, gradient cannot be obtained at these points. An advantage of the DSGA algorithm is that the technique still works for these types of non-differentiable functions simply by replacing gradient with sub-gradient, which exists at all points for the introduced objective function [13].

For the micro-sources that are present in configuration C_i (whose power we denote with $P^m_{MS}(t, C_i)$) and are able to contribute to system resiliency, the sub-gradient consists of the sub-derivatives of components of (29) with respect to decision variables:

$$\frac{\partial P^m_{Def}(t, C_i)}{\partial P^m_{MS}(t, C_i)} = \mathbb{I}\Big\{P^m_f(t) \geq P^m_{DG}(t, C_i) + P^m_{PV}(t) + P^m_{ESS}(t, C_i) + P^m_G(t, C_i) + P^m_C(t)\Big\} \tag{36}$$

where, $\mathbb{I}\{\cdot\}$ is the indicator function with respect to input S, defined as follows:

$$\mathbb{I}\{S\} = \begin{cases} 1 & if\ S\ is\ True \\ 0 & if\ S\ is\ False \end{cases} \tag{37}$$

Note that the sub-derivative (36) basically states that the remaining micro-sources in a certain configuration should increase their output power to compensate for power deficiency in generation outage, ESS failure, or islanding scenarios. Using the indicator function and the simple fact that $\min(a, b) = 0.5*(a + b - |a - b|)$, the sub-derivatives of power reserve with respect to different decision variables can be calculated from Eqs. (32)–(35), as:

$$\frac{\partial P^m_{DG,Res}(t, C_i)}{\partial P^m_{DG}(t, C_i)} = -\mathbb{I}\left\{P^{\max,m}_{DG}(t) - P^m_{DG}(t, C_i) \leq GRC^m \cdot \Delta t\right\} \tag{38}$$

$$\frac{\partial P^m_{G,Res}(t, C_i)}{\partial P^m_G(t, C_i)} = -1 \tag{39}$$

$$\frac{\partial P^m_{C,Res}(t, C_i)}{\partial P^m_C(t, C_i)} = -1 \tag{40}$$

$$\frac{\partial P^m_{ESS,Res}(t, C_i)}{\partial P^m_{ESS}(t, C_i)} = -1 \tag{41}$$

$$\frac{\partial P^m_{ESS,Res}(t, C_i)}{\partial P^m_{ESS}(t', C_i)} = -\mathbb{I}\left\{P^{\max,m}_{ESS} - P^m_{ESS}(t, C_i), \frac{E(t, C_i) - E^{\min,m}}{\Delta t}\right\}, \quad (for\ t < t') \tag{42}$$

Intuitively, Eqs. (38)–(42) tend to prevent the micro-sources from being deployed up to their full capacity, in order to make room for sufficient power reserve in case there is an emergency.

Using Eq. (36) along with (38)–(42), we obtain the total sub-gradient of objective function (29) with respect to the decision vector $\boldsymbol{P}$ in (27). This sub-gradient is then inserted in the DSGA to complete the algorithm, as described in the next section.

4. SOLUTION METHODOLOGY

The DSGA can be employed to solve (27) through a distributed optimization framework, as demonstrated in [12–14]. Within the distributed bargaining framework, the agents exchange their estimation of the location of NBS

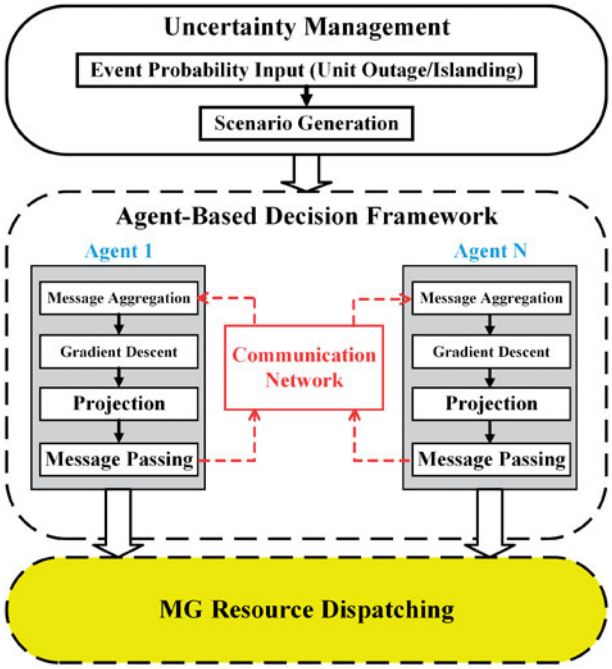

FIGURE 3. Overall agent-based control system.

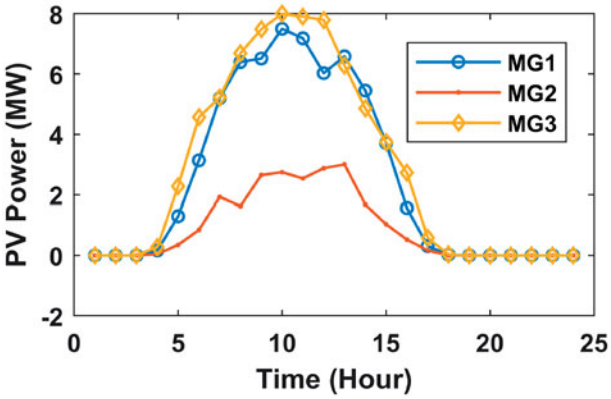

FIGURE 4. PV power data for different MGs.

with each other. These exchanged estimations are referred to as "messages" in this section. The DSGA consists of the following steps, that the agents perform at each iteration of the algorithm:

- **Message aggregation:** The agent aggregates the received messages from its neighboring agents using a weighted averaging operation:

$$\boldsymbol{\omega_i(k)} = \sum_{l=1}^{Ne_i} a_i^l \boldsymbol{P_l(k)} \tag{43}$$

where, Ne_i denotes the i^{th} agent's number of neighboring agents (including the i^{th} agent).

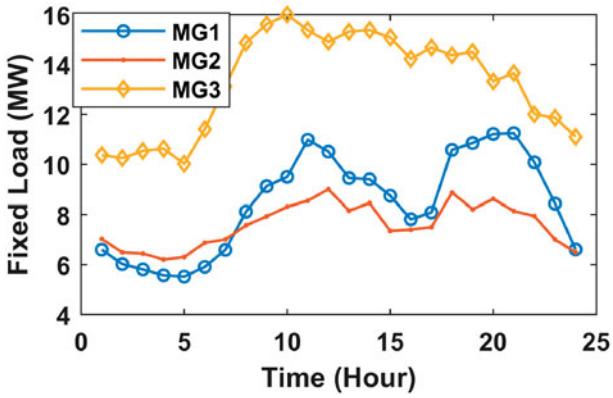

FIGURE 5. Fixed load profiles of MGs.

- **Gradient descent:** The agent improves the aggregated message by performing gradient descent with respect to its objective function or the set of objective functions:

$$\boldsymbol{v_i(k)} = \boldsymbol{\omega_i(k)} - \alpha_k \cdot \nabla_{P_i} f_i(\boldsymbol{P_i(k)}) \tag{44}$$

where, α_k is a time-varying weight factor. The gradient of the cost function for the NBS formulation (27) is obtained as follows:

$$\nabla_{\boldsymbol{P}} f_i(\boldsymbol{P}) = -\begin{bmatrix} \frac{\partial U_{1,i}^m}{\partial P_1} & \cdots & \frac{\partial U_{O_i^m,i}^m}{\partial P_L} \\ \vdots & \ddots & \vdots \\ \frac{\partial U_{1,i}^m}{\partial P_1} & \cdots & \frac{\partial U_{O_i^m,i}^m}{\partial P_L} \end{bmatrix} \cdot \begin{bmatrix} \frac{1}{U_{1,i}^m - d_{1,i}^m} \\ \vdots \\ \frac{1}{U_{O_i^m,i}^m - d_{O_i^m,i}^m} \end{bmatrix} \tag{45}$$

- **Projection:** The agent projects the obtained estimated solution into its local feasible operational region, defined by its local/global constraints:
-

$$\mathbf{P_i(k+1)} = \mathcal{P}_{X_i}[\boldsymbol{v_i(k)}] \tag{46}$$

where, $\mathcal{P}_{X_i}$ defines the projection operation into the set X_i. Note that the projection operation is a convex quadratic programing problem [25], which is formulated as follows:

$$\mathcal{P}_{X_i}[\boldsymbol{v_i(k)}] = arg \min_{\boldsymbol{y} \in X_i} |\boldsymbol{y} - \boldsymbol{v_i(k)}| \tag{47}$$

where, $|\cdot|$ is the Euclidean norm.

- **Message transmission:** The agent sends the updated estimation back to its neighbors.

Considering the convexity of the decision model (17), DSGA is guaranteed to converge to the NBS of the bargaining game. A flow diagram of the proposed decision framework is shown in Figure 3.

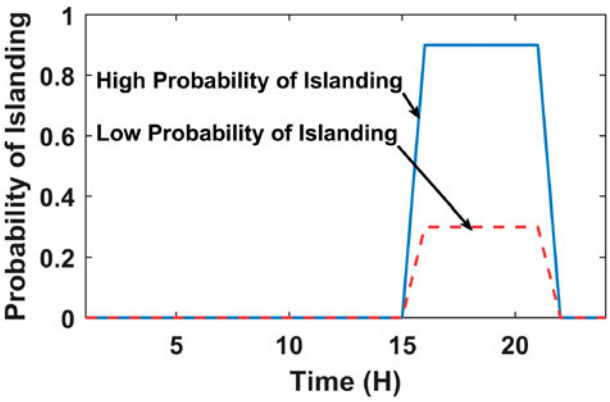

FIGURE 6. Probability of MG islanding.

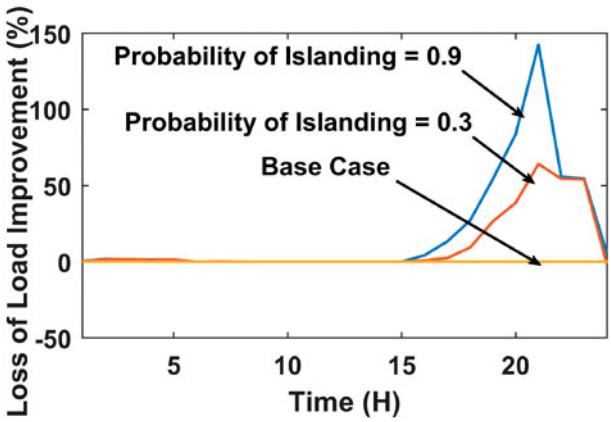

FIGURE 7. Improvements in the expected power deficit under different islanding scenarios.

5. SIMULATION RESULTS AND DISCUSSION

The proposed power management model is tested on a distribution system consisting of three MGs, with each MG being a modified version of the IEEE 13-bus standard distribution network [11]. Note that the MGs are not identical, and have micro-sources with different nominal capacities and outputs [14]. PV power profiles of the MGs have been obtained from [26], and shown in Figure 4. Figure 5 shows the fixed load data for the MGs, which are adopted from [27] and [28]. In this paper, the retail price is assumed to be \$90/MWh at all times of the day. Note that in this paper, the effect of variable and dynamic pricing in the market has not been considered. The objective is to exclusively study system resiliency without market interference. For a thorough analysis of the proposed agent-based model in market environment refer to [14].

Three case studies are considered: in Case I, the behavior of MGs is investigated when a blackout in the main grid is expected due to high probability of an extreme event. In Case II, a high failure probability is assigned to a DG unit in one of the MGs for a certain time period and the reaction of the power management strategy to the probable unit failure scenario is investigated. Hence, in both of these cases, the power management predicts how to "prepare" the system for a certain look-ahead time in the pre-event state, based on the forecasted probabilities for the occurrence of different events (*e.g.*, islanding or unit failure) with the objective of minimizing post-outage power loss. In Case III, the behavior of an islanded MG under ESS failure scenario is studied, with a focus on the load voltage profile.

Case I: Probable Grid Blackout Due to an Extreme Event

In Figure 6, the estimated islanding probability of the MGs is shown during a certain time interval of day for two scenarios. These probability values are estimated by the expert system or given as input to the optimization problem by the owner/operator of each MG, as described in Section III. As can be seen in this figure, at the time interval 16:00–21:00, the probability of islanding jumps to 0.3 in one scenario (mild possibility of grid blackout), and to 0.9 in another scenario (severe possibility of disruption with almost certain blackout in the main grid). The distributed optimization framework has been run under these two scenarios. The improvement levels in the expected loss of load (compared to the case where resiliency-awareness is not built into the decision model) are shown in Figure 7. As shown in this figure, the percentage improvement level in expected loss of load is considerably higher as the probability of islanding increases. This implies higher levels of self-sufficiency in operation of the MGs during islanding.

To verify the performance of the resiliency-aware distributed power management scheme it is crucial to compare the performance of the system with and without the proposed objective function. Hence, tests have been run for these two cases, where in both cases an islanding probability of 0.9 is forecasted for time interval 16:00–21:00 for all the three MGs (as shown in Figure 6). The value of total reserve from the micro-sources of all the three MGs is shown in Figure 8. As can be seen in this figure, when the resiliency-aware functionality is built into the power management system, higher reserve values are maintained during the times that islanding is expected.

A significant portion of the higher power reserve during the higher probability of extreme event (islanding) is due to change in operation of ESS units of the MGs. In Figure 9, the total stored energy level of all the ESS units in the distribution system is shown at different times of day. It can be

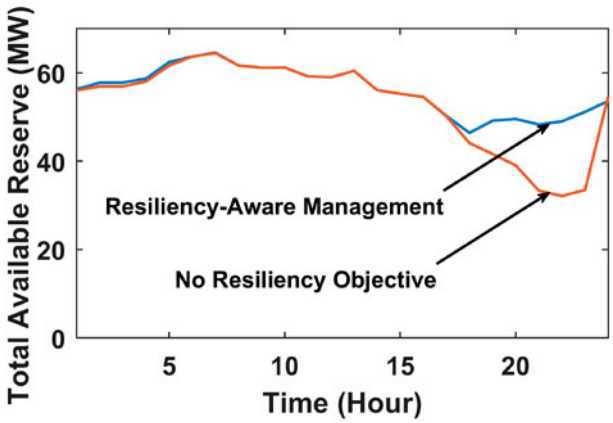

FIGURE 8. Reserve allocation with and without resiliency-aware functionality.

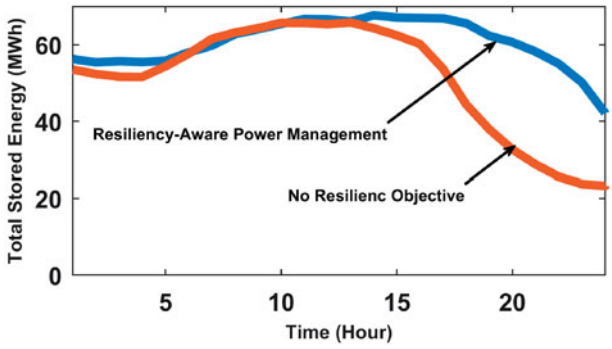

FIGURE 9. Total stored energy in the ESS units within the MGs.

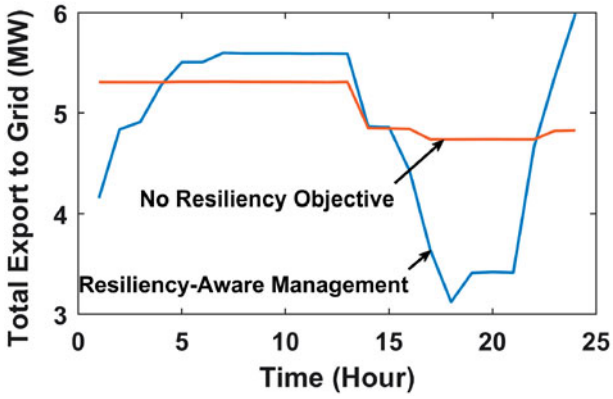

FIGURE 10. Total power export to the main grid.

observed, that employing the resiliency-aware functionality leads to higher stored energy levels, especially at critical times of day, when higher chances of islanding is expected. Note that higher stored energy implies higher available power reserve levels.

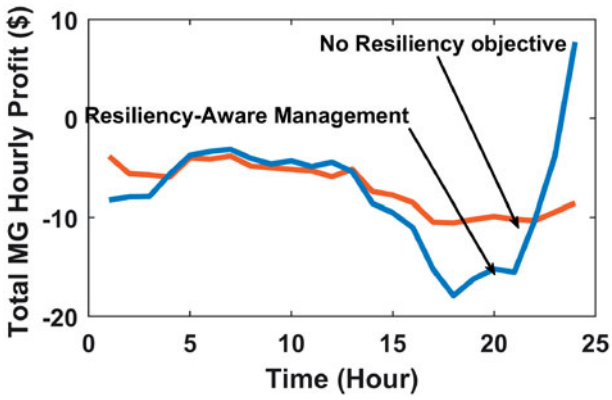

FIGURE 11. Hourly profit level of all MGs through sales of power to the grid.

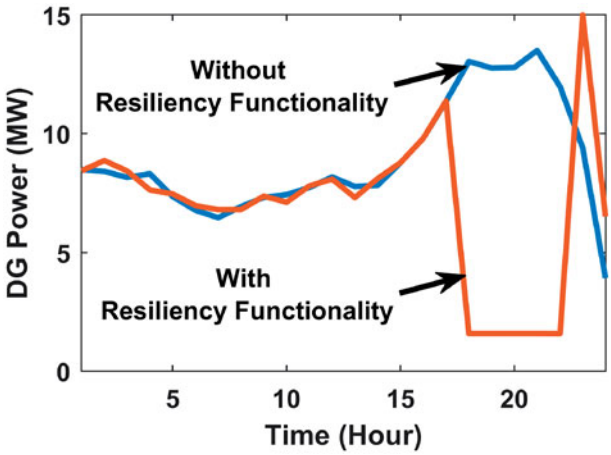

FIGURE 12. Power output of MG1's DG.

Another interesting aspect of the system operation with the resiliency-aware functionality is that introducing the proposed objective function leads to lower power export to the grid during the critical time interval 16:00–21:00 to prepare for islanding, as demonstrated in Figure 10. This reduction in the export is due to higher concentration on reserve allocation, which leads to reduced reliance on the grid. On the other hand, lower power export to the grid leads to a loss of revenue for the MGs, which is usually not the focus at times of crisis. Figure 11 shows the aggregate hourly profit of the MGs with and without the resiliency-aware functionality. As is demonstrated here, resiliency-awareness leads to a decrease in the profit level, at the time interval where a blackout in the main grid is expected. The total loss of profit is equal to 9.3% compared to the base case without the proposed objective function. This suggest that there is a tradeoff between the two objective functions of resiliency-awareness and short-term profit.

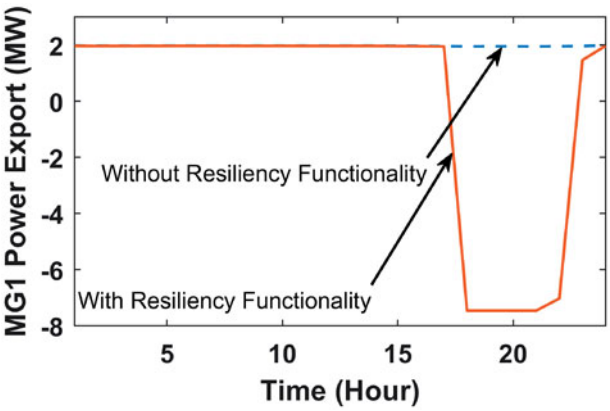

FIGURE 13. MGs' power export to the grid.

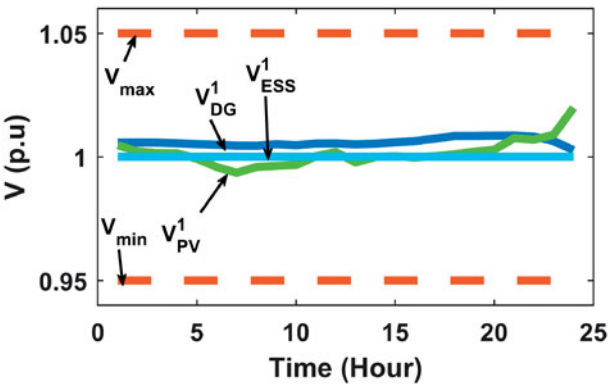

FIGURE 14. Voltage magnitude of buses.

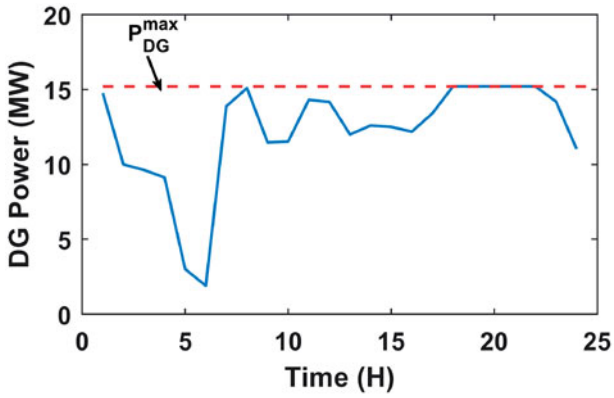

FIGURE 15. DG output (ESS failure scenario).

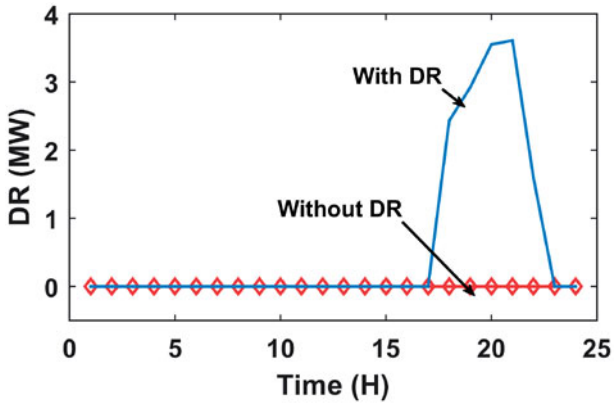

FIGURE 16. DR (ESS failure scenario).

Case II: Probable Unit Failure Scenario

In Case I, we assigned a near-zero probability to unit failure events. For Case II, we assume that the DG unit in MG1 has a high probability of failure (equal to 0.9) during the peak load hours 18:00–22:00 (Figure 5). The power profile of the DG unit for MG1, with and without the resiliency functionality, is shown in Figure 12. As can be seen in this figure, introducing the resiliency-aware functionality leads to significant drop in the DG unit output power during the critical time interval, when the failure is expected. Due to the decreased power output from the DG unit, MG1 needs to rely on other MGs and the main grid to maintain the local load balance. The aggregate hourly power export profile of the MGs to the main grid is shown in Figure 13. As is observed in this figure, for the case with resiliency-aware functionality, MGs start buying (importing) power from the main grid during the critical time interval to compensate for the lower power output from the DG unit of MG1, as expected. For the case without resiliency-aware functionality, power export from the MGs to the grid continues during the critical time interval. Hence, we can conclude that the inclusion of the proposed objective function (29) in the power management algorithm is able to prepare the MGs for expected (predicted) unit failure events, by changing the output power of the micro-sources in favor of the healthier units.

Case III: Islanding and Unit Failure Scenario

In this section we study the behavior of islanded MG1 with healthy units and under a unit failure scenario. The voltage profile of the islanded MG without unit failure is shown in Figure 14. As can be seen in this figure the voltage level of all the micro-source buses are kept within permissible bounds (1 ± 0.05 p.u) at all times. Now we assume an ESS unit failure occurs at time 9:00.

Initially, the DG unit along with the PV system are able to supply the MG load and maintain the system power balance by load following, as observed in Figure 15. However, during the later hours of the day (17:00–22:00) when a secondary peak occurs in the load profile of MG1, (Figure 5), and PV power is not available, the DG unit

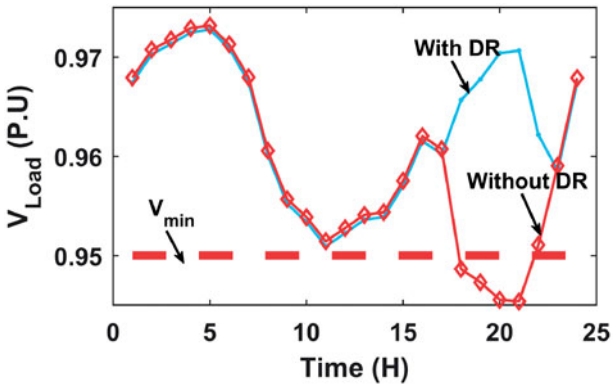

FIGURE 17. Load voltage profile.

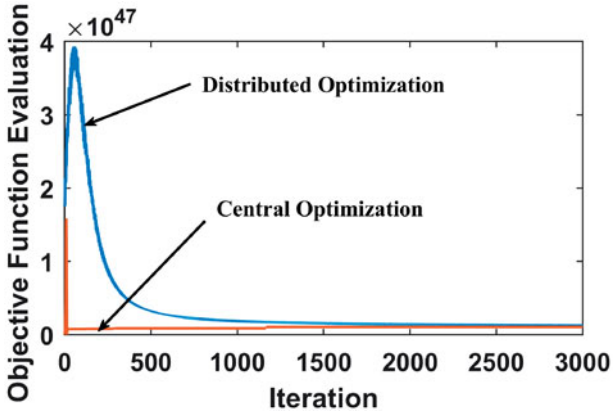

FIGURE 18. Model comparison: distributed optimization (proposed) vs. central optimization [14].

alone is not able to maintain the power balance in the system. As can be seen in Figure 15, the DG output power reaches its maximum level, indicating that the total reserve from the micro-sources is exploited. To maintain the power balance in this interval, DR resources are employed as depicted in Figure 16. This case shows the use of limited load shedding during critical time intervals, when power reserve is not available in the system from local generation units.

The employment of DR resources has a direct effect on the voltage profile at the load bus in which DR resources are available. As depicted in Figure 17, without using DR resources the voltage of the load feeder drops below the minimum permissible limit, during the critical peak load interval, while the employment of DR resources keeps the bus voltage within the limits.

5.1. Comparison with conventional approaches

The performance of the proposed optimization framework is compared with conventional central optimization approaches [14]. As shown in Figure 18, both the proposed distributed method and the conventional method converge to the same unique NBS. The proposed model takes more iteration to converge, however, it is much faster compared to the central method (*i.e.*, it has less computational load per iteration.) Also, it was observed that the proposed model scales better than the central approach. Hence, as we increase the size of the system we can solve for the NBS much faster when using the agent-based model instead of a conventional algorithm.

6. CONCLUSIONS

In this paper, we have proposed a resiliency-aware power management approach, to prepare the system for extreme events and unit failure, considering multiple MGs in a power distribution network. The proposed agent-based method is based on a fully distributed cooperative resource allocation scheme which attempts to maintain bus voltages within the permissible limit. NBS is used as a solution concept for the decision model. To improve the resiliency of the system, a probabilistic objective function is introduced into the cooperative reserve allocation problem of the MGs, which minimizes the expected net power deficit for each MG and prepares the system for improved performance during expected extreme events. The numerical results show that the proposed model is able to reduce the power deficit during critical times and contribute to the resiliency of the system.

FUNDING

This work was supported by Montana State University, and the U.S. Department of Energy, Office of Science, Basic Energy Sciences, under Award # DE-FG02-11ER46817.

REFERENCES

[1] S. Chanda and A. K. Srivastava, "Defining and enabling resiliency of electric distribution systems with multiple microgrids," *IEEE Trans. Smart Grid*, vol. 7, no. 6, pp. 2859–2868, Nov. 2016.

[2] R. Arghandeh, A. von Meier, L. Mehrmanesh, and L. Mili, "On the definition of cyber-physical resilience in power systems," *Renew. Sustain. Energy Rev.*, vol. 58, pp. 1060–1069, 2016.

[3] "The US National Academies of Sciences, Engineering, and Medicine report: Enhancing the resilience of the nations electricity system - 2017," Available: http://www.nap.edu/24836.

[4] J. Chen and Q. Zhu, "A game-theoretic framework for resilient and distributed generation control of renewable energies in microgrids," *IEEE Trans. Smart Grid*, vol. 8, no. 1, pp. 285–295, Jan. 2017.

[5] A. Gholami, T. Shekari, F. Aminifar, and M. Shahidehpour, "Microgrid scheduling with uncertainty: the quest for resilience," *IEEE Trans. Smart Grid*, vol. 7, no. 6, pp. 2849–2858, Nov. 2016.
[6] X. Liu, M. Shahidehpour, Z. Li, X. Liu, Y. Cao, and Z. Bie, "Microgrids for enhancing the power grid resilience in extreme conditions," *IEEE Trans. Smart Grid*, vol. 8, no. 2, pp. 589–597, Mar. 2017.
[7] K. P. Schneider, F. K. Tuffner, M. A. Elizondo, C. C. Liu, Y. Xu, and D. Ton, "Evaluating the feasibility to use microgrids as a resiliency resource," *IEEE Trans. Smart Grid*, vol. 8, no. 2, pp. 687–696, Mar. 2017.
[8] E. Pashajavid, F. Shahnia, and A. Ghosh, "Development of a self-healing strategy to enhance the overloading resilience of islanded microgrids," *IEEE Trans. Smart Grid*, vol. 8, no. 2, pp. 868–880, Mar. 2017.
[9] A. Khodaei, "Resiliency-oriented microgrid optimal scheduling," *IEEE Trans. Smart Grid*, vol. 5, no. 4, pp. 1584–1591, Jul. 2014.
[10] Z. Wang, B. Chen, J. Wang, and C. Chen, "Networked microgrids for self-healing power systems," *IEEE Trans. Smart Grid*, vol. 7, no. 1, pp. 310–319, Jan. 2016.
[11] K. Dehghanpour and H. Nehrir, "Real-time multiobjective microgrid power management using distributed optimization in an agent-based bargaining framework," *IEEE Trans. Smart Grid*, 2018. DOI: 10.1109/TSG.2017.2708686 [Online]. Available: https://ieeexplore.ieee.org/stamp/stamp.jsp?tp=&arnumber=7934324.
[12] A. Nedic and A. Ozdaglar, "Distributed subgradient methods for multiagent optimization," *IEEE Trans. Automat. Control*, vol. 54, no. 1, pp. 48–61, Jan. 2009.
[13] A. Nedic, A. Ozdaglar, and P. A. Parrilo, "Constrained consensus and optimization in multi-agent networks," *IEEE Trans. Automat. Control*, vol. 55, no. 4, pp. 922–938, Apr. 2010.
[14] K. Dehghanpour and H. Nehrir, "An agent-based hierarchical bargaining framework for power management of multiple cooperative microgrids," *IEEE Trans. Smart Grid*, 2018. DOI: 10.1109/TSG.2017.2746014 [Online]. Available: https://ieeexplore.ieee.org/stamp/stamp.jsp?tp=&arnumber=8017431.
[15] S. S. Guggilam, E. Dall'Anese, Y. C. Chen, S. V. Dhople, and G. B. Giannakis, "Scalable optimization methods for distribution networks with high PV integration," *IEEE Trans. Smart Grid*, vol. 7, no. 4, pp. 2061–2070, Jul. 2016.
[16] M. Maschler, E. Solan, and S. Zamir, *Game Theory*. Cambridge, UK: Cambridge University Press, 2013.
[17] C. Yang, A. A. Thatte, and L. Xie, "Multitime-scale data-driven spatiotemporal forecast of photovoltaic generation," *IEEE Trans. Sustain. Energy*, vol. 6, no. 1, pp. 104–112, Jan. 2015.
[18] A. Pourmousavi, M. H. Nehrir, and R. K. Sharma, "Multi-timescale power management for islanded microgrids including storage and demand response," *IEEE Trans. Smart Grid*, vol. 6, no. 3, pp. 1185–1195, May 2015.
[19] S. Bolognani and S. Zampieri, "On the existence and linear approximation of the power flow solution in power distribution networks," *IEEE Trans. Power Syst.*, vol. 31, no. 1, pp. 163–172, Jan. 2016.
[20] Q. Peng, Y. Tang, and S. H. Low, "Feeder reconfiguration in distribution networks based on convex relaxation of OPF," *IEEE Trans. Power Syst.*, vol. 30, no. 4, pp. 1793–1804, Jul. 2015.
[21] Z. M. Fadlullah, D. M. Quan, N. Kato, and I. Stojmenovic, "GTES: an optimized game-theoretic demand-side management scheme for smart grid," *IEEE Syst. J.*, vol. 8, no. 2, pp. 588–597, Jun. 2014.
[22] M. Ross, C. Abbey, F. Bouffard, and G. Joos, "Multiobjective optimization dispatch for microgrids with a high penetration of renewable generation," *IEEE Trans. Sustain. Energy*, vol. 6, no. 4, pp. 1306–1314, Oct. 2015.
[23] M. Panteli, D. N. Trakas, P. Mancarella, and N. D. Hatziargyriou, "Boosting the power grid resilience to extreme weather events using defensive islanding," *IEEE Trans. Smart Grid*, vol. 7, no. 6, pp. 2913–2922, Nov. 2016.
[24] J. Dupacova, N. Growe-Kuska, and W. Romisch, "Scenario reduction in stochastic programming," *Math. Program.*, vol. 95, no. 3, pp. 493–511, Mar. 2003.
[25] S. Boyd and N. Vandenberghe, *Convex Optimization*. New York: Cambridge University Press, 2009.
[26] "Electric Power Research Institute (EPRI): Distributed PV monitoring and feeder analysis - Jun. 2012," Available: http://dpv.epri.com/measurement data.html.
[27] NREL, "Randomized hourly load data for use with taxonomy distribution feeders," Available: https://catalog.data.gov/harvest/object/, Nov. 2015.
[28] A. Hoke, R. Butler, J. Hambrick, and B. Kroposki, "Steady-state analysis of maximum photovoltaic penetration levels on typical distribution feeders," *IEEE Trans. Sustain. Energy*, vol. 4, no. 2, pp. 350–357, Apr. 2013.

BIOGRAPHIES

Kaveh Dehghanpour received his B.Sc. and M.S. from University of Tehran in electrical and computer engineering, in 2011 and 2013, respectively. He received his Ph.D. in electrical engineering from Montana State University in 2017. He is currently a postdoctoral research associate at Iowa State University. His research interests include application of machine learning and data-driven techniques in power system monitoring and control.

Hashem Nehrir received the B.S., M.S., and Ph.D. degrees from Oregon State University, Corvallis, OR, USA, in 1969, 1971, and 1978, respectively, all in electrical engineering. He is a Professor in the Department of Electrical and Computer Engineering at Montana State University, Bozeman, MT, USA. His research interests include modeling and control of power systems, alternative energy power generation systems, and application of intelligent controls to power systems. He is the author of three textbooks and an author or coauthor of numerous technical papers. He is a Life Fellow of IEEE and the recipient of IEEE-PES Ramakumar Family Renewable Energy Excellence Award in 2016.